

# GI Supply now offers complete motility and reflux management systems.



## SOLAR GI™ HIGH RESOLUTION MANOMETRY



Economical and Customizable



Latest Chicago and London Classifications



Wide Range of Standard and Customizable Catheters

## OHMEGA™ AMBULATORY IMPEDANCE-PH RECORDER



Complete Reflux Management System



Easy to Use Software



Wide Range of Catheters

# VISIT US AT ANMS BOOTH 10

**For More Information or Support**

Call: (800) 451-5797 Visit: [www.gi-supply.com](http://www.gi-supply.com)




Solar GI and Ohmega are trademarks of Laborie Medical Technologies Corp.  
Disclaimer: GI Supply is an authorized distributor of Laborie Medical Technologies Corp. in The United States of America

G-1915-01 | © 2021 GI Supply, Inc. | All rights reserved.

 **GI Supply**<sup>®</sup>  
Specialty Endoscopic Products



# Supernatants of intestinal luminal contents from mice fed high-fat diet impair intestinal motility by injuring enteric neurons and smooth muscle cells

Yvonne Nyavor<sup>1</sup>  | Catherine R. Brands<sup>1</sup> | Jessica Nicholson<sup>1</sup> | Sydney Kuther<sup>1</sup> | Kortni K. Cox<sup>1</sup> | George May<sup>1</sup> | Christopher Miller<sup>1</sup> | Allysha Yasuda<sup>1</sup> | Forrest Potter<sup>1</sup> | Joshua Cady<sup>1</sup> | Heino M. Heyman<sup>2</sup>  | Thomas O. Metz<sup>2</sup> | Timo D. Stark<sup>3</sup> | Thomas Hofmann<sup>3</sup> | Onesmo B. Balemba<sup>1</sup> 

<sup>1</sup>Department of Biological Sciences, University of Idaho, Moscow, ID, USA

<sup>2</sup>Earth and Biological Sciences Directorate, Pacific Northwest National Laboratory, Richland, WA, USA

<sup>3</sup>Lehrstuhl für Lebensmittelchemie und Molekulare Sensorik, Technische Universität München, Freising, Germany

## Correspondence

Onesmo B. Balemba, Department of Biological Sciences, University of Idaho, 875 Perimeter Drive, LSS 252, Moscow, ID 83844, USA.  
Email: obalemba@uidaho.edu

## Funding information

This study was supported by the University of Idaho—Dyess Faculty Fellowship and National Institutes of Health grant number S10OD018044 to Deborah Stenkamp. Additional support was by Institutional Development Awards (IDeA) from the National Institute of General Medical Sciences of the National Institutes of Health under grant numbers P20 RR016454 and the National Center for Research Resources grant number P20 GM103408 through IDAHO INBRE.

## Abstract

**Background:** Damage to enteric neurons and impaired gastrointestinal muscle contractions cause motility disorders in 70% of diabetic patients. It is thought that enteric neuropathy and dysmotility occur before overt diabetes, but triggers of these abnormalities are not fully known. We tested the hypothesis that intestinal contents of mice with and without high-fat diet- (HFD-) induced diabetic conditions contain molecules that impair gastrointestinal movements by damaging neurons and disrupting muscle contractions.

**Methods:** Small and large intestinal segments were collected from healthy, standard chow diet (SCD) fed mice. Filtrates of ileocecal contents (ileocecal supernatants; ICS) from HFD or SCD mice were perfused through them. Cultured intact intestinal muscularis externa preparations were used to determine whether ICS and their fractions obtained by solid-phase extraction (SPE) and SPE subfractions collected by high-performance liquid chromatography (HPLC) disrupt muscle contractions by injuring neurons and smooth muscle cells.

**Key Results:** ICS from HFD mice reduced intestinal motility, but those from SCD mice had no effect. ICS, aqueous SPE fractions and two out of twenty HPLC subfractions of aqueous SPE fractions from HFD mice blocked muscle contractions, caused a loss of nitrergic myenteric neurons through inflammation, and reduced smooth muscle excitability. Lipopolysaccharide and palmitate caused a loss of nitrergic myenteric neurons but did not affect muscle contractions.

**Conclusions & Inferences:** Unknown molecules in intestinal contents of HFD mice trigger enteric neuropathy and dysmotility. Further studies are required to identify the toxic molecules and their mechanisms of action.

**Abbreviations:** ALC10 +11, HPLC subfractions 10 and 11 of the aqueous SPE1 fractions of ICS; ANNA1, anti-neuronal nuclear antibody 1; DHE, dihydroethidium; ENS, enteric nervous system; GI, gastrointestinal; GS, anti-glutathione synthase antibody; HFD, high-fat diet; HFD-ICS, ileocecal supernatants from HFD mice; HFD-SPE1, aqueous solid-phase extraction fraction of HFD-ICS; HPLC, high-performance liquid chromatography; ICS, ileocecal supernatants; IJPs, inhibitory junction potentials; IL-6, Interleukin 6; iNOS, inducible nitric oxide synthase; LPS, lipopolysaccharide; MCP1, monocyte chemo-attractant protein 1; MLC1, HPLC subfraction 1 of the methanolic SPE4 fractions of ICS; nNOS, neuronal nitric oxide synthase; PAI-1, plasminogen activator inhibitor-1; SCD-SPE1, aqueous solid-phase extraction fraction of SCD-ICS; SCD, standard chow diet; SCD-ICS, ileocecal supernatants from SCD mice; SMCs, smooth muscle cells; SPE, solid-phase extraction; T2D, type 2 diabetes; TNF $\alpha$ , Tumor necrosis factor-alpha; VIP, vasoactive intestinal peptide.

## KEYWORDS

diabetic neuropathy, dysmotility, lipopolysaccharide, nNOS neurons, palmitate

## 1 | INTRODUCTION

It is estimated that 50% of the greater than 400 million people with type 2 diabetes (T2D)<sup>1</sup> suffer from debilitating complications caused by neuropathy.<sup>2</sup> Such complications include gastrointestinal (GI) motility disorders<sup>3</sup> which are dysphagia, gastroparesis, constipation, diarrhea, incontinence, and pain.<sup>4,5</sup> These diabetic GI motility-related disorders are caused by neuropathy in the enteric nervous system (ENS) and smooth muscle dysfunction.<sup>6,7</sup> The major ENS injuries associated with diabetic dysmotility include loss of nitrergic myenteric neurons, which co-express neuronal nitric oxide synthase (nNOS) plus vasoactive intestinal peptide (VIP), axonal swelling, and loss of cytoskeletal filaments.<sup>4,8,9</sup>

Diabetic GI motility disorders and ENS neuropathy are commonly thought to be caused by oxidative stress, advanced glycation end products, and sorbitol accumulation in neurons<sup>4,10</sup> elicited by hyperglycemia, hyperlipidemia, microvascular damage, and inflammation.<sup>4,11</sup> However, recent studies suggest that GI dysmotility and associated ENS neuropathy develop before hyperglycemia and insulin resistance.<sup>12,13</sup> Saturated fatty acids (palmitate in particular), microbial metabolites, and bacterially derived lipopolysaccharide (LPS) are thought to be responsible triggers.<sup>12,14-16</sup> It is thought that LPS and palmitate act synergistically to trigger damage in ENS nerve cells. This suggests that diet-bacteria-host interactions have a crucial role in the pathophysiology of GI diabetic neuropathy and dysmotility.<sup>12,17</sup> However, knowledge of other potentially toxic molecules from GI luminal contents and the mechanisms responsible for triggering ENS neuropathy and GI dysmotility in prediabetes, T2D, and other motility-related disorders is limited.

HFD animal models are used to study T2D and diabetic neuropathy because T2D is commonly associated with consuming a high-fat western diet.<sup>18</sup> In addition, high-fat diet (HFD) ingestion and T2D are also associated with gut microbiota changes<sup>19</sup> and dysmotility.<sup>12,13</sup> HFD-induced diabetic ENS injuries in laboratory mice and rats correspond with ENS injuries in T2D humans.<sup>8,18</sup> We previously showed that GI dysmotility and a loss of nitrergic myenteric neurons occur in male and female C57BL/6 mice fed a HFD for 8 weeks.<sup>8,13</sup> The aim of this study was to test hypothesis that toxic molecules other than LPS and palmitate from the GI luminal contents trigger diabetic GI dysmotility and ENS neuropathy by damaging smooth muscle and enteric neurons. This was achieved by determining whether ileocecal contents from mice fed HFD trigger dysmotility by damaging nitrergic myenteric neurons and disrupting smooth muscle function and beginning to identify the toxic molecules.

### Key Points

- There is a growing interest in identifying neurotoxic and antimotility substances originating from the gut, because these substances could cause neurodegeneration and cardiovascular complications in diabetes and other major illnesses. By using a high-fat diet mouse model, we show that contents from the distal ileum and cecum of mice fed high-fat diet (HFD) contain unknown toxic molecules that impair intestinal motility by damaging enteric neurons and smooth muscle cells, and disrupting their functions. Also, sera from HFD mice reduced muscle contractions.
- The unknown neurotoxic and antimotility molecules impair intestinal motility by damaging nitrergic myenteric neurons, disrupting inhibitory neuromuscular transmission, and inhibiting the excitability of smooth muscle cells.
- Neurotoxic and antimotility molecules in ileocecal contents of HFD mice damage enteric neurons, smooth muscle, and other cells in the intestinal muscle layer via inflammation and nitrosative stress.
- These initial results suggest that the neurotoxic and antimotility molecules in ileocecal contents of HFD mice are likely aqueous and can be isolated using solid-phase chromatography and high-performance liquid chromatography.

## 2 | MATERIALS AND METHODS

### 2.1 | Mice

The University of Idaho Animal Care and Use Committee approved study procedures. Six to seven weeks old male and female C57Bl/6J mice from Jackson Laboratories (Bar Harbor, ME) were housed on a 12-h light cycle with ad libitum access to food and water. At 8 weeks, mice were split into two groups and fed either a standard chow diet (SCD) composed of 6.2% kcal fat (Teklad Global 2018, Teklad Diets, Madison WI) or a HFD containing 72% fat (70% kcal fat diet with 2% additional corn oil; TestDiet, Richmond, IN) for 8 weeks.<sup>13</sup> Male and female mice were used for initial motility experiments and serum studies. Male mice were used for all other experiments. For

experiments with dihydroethidium (DHE), we used first generation of GCaMP6f mice obtained by crossing female B6J.Cg-Gt(ROSA)26Sor<sup>tm95.1(CAG-GCaMP6f)Hze</sup>/MwarJ (Stock no. 028865) mice with male B6.129-Nos1<sup>tm1(cre)Mgmj</sup>/J (Stock no. 017526) purchased from the Jackson Laboratories. GCaMP6f green fluorescence in nNOS neurons enabled us to readily visualize and photograph myenteric ganglia in live tissues to analyze DHE. These mice were fed SCD. Mice were euthanized by exsanguination after deep isoflurane anesthesia. Contents from cecum and 3 cm long distal ileum (ileocecal contents) were collected from HFD and SCD mice into sterile 2.0 ml Eppendorf tubes and stored at  $-80^{\circ}\text{C}$ . We used ileocecal contents to get adequate amounts for motility assays by assuming that peristalsis move contents from terminal ileum into cecum during death. Cecum contents constituted over 90% of the contents.

## 2.2 | Motility assays to determine whether ileocecal supernatants (ICS) affect intestinal propulsion

Motility assays were conducted using the Gastrointestinal Motility Monitoring system to record duodenal contractions and pellet propulsion as previously described.<sup>13</sup> Samples were equilibrated for 30 min. Four baseline videos were obtained during intraluminal superfusion with Krebs at a flow rate of 0.5 ml/min through cannulated duodenojejunal segments (duodenum +5.0 cm proximal jejunum or entire colon). Ileocecal contents from both male and female HFD and SCD mice were weighed and subsequently suspended in Krebs at a ratio of 1:100 weight/volume. We used this ratio for all subsequent experiments. Solid materials were filtered out with a Whatman filter paper to obtain non-sterile ICS, which were superfused into isolated intestinal segments at a similar flow rate and videos recorded. Next, ICS were sterile filtered with 0.22  $\mu\text{m}$  filters and sterile ICS tested in a similar manner. We tested ICS from male mice on samples from male mice and tested ICS from female mice on samples from female mice to avoid potential effects due to gender. The effect of HFD itself was tested by a suspension of HFD in Krebs. Duodenal contraction and pellet propulsion velocities were calculated using established procedures.<sup>13</sup> See supplementary information for details.

## 2.3 | Separating ICS into fractionations by solid-phase extraction (SPE)

Sterile ICS from male HFD and SCD mice were freeze-dried. Aliquots were separated by standard SPE fractionation into 100% water fraction (hereafter, SPE1), 20% methanol (SPE2), 50% methanol (SPE3), and 100% methanol (SPE4) using a previously published procedure.<sup>20</sup> A detailed procedure can be found in the supplementary information.

## 2.4 | Separating SPE1 and SPE4 into subfractions by high-performance liquid chromatography (HPLC)

In pilot assays, SPE1 reduced duodenal propulsive contractions after 5 min and blocked contractions of cultured duodenal muscularis after 6–12 h. SPE4 did not affect duodenal propulsive contractions after 10 min but reduced muscularis contractions after 24 h. SPE2-3 did not affect duodenal propulsive contractions and muscularis contractions. Therefore, SPE1 and SPE4 from HFD and SCD mice were subfractionated by using HPLC into 20 subfractions, each. The information about the equipment, reagents, and procedure is in the supplementary information. To obtain enough amounts (1:100 weight/volume) for bioactivity assays, HPLC subfractions 10 and 11 from the aqueous SPE1 (here after, ALC10-11) were combined. HPLC subfraction 1 of the methanolic SPE4 (here after, MLC1) was the only subfraction collected in sufficient amounts for bioactivity assays. Therefore, freeze-dried SPE1, SPE4 fractions and their respective ALC10-11 and MLC1 subfractions were the only samples analyzed using muscularis contraction, nerve cell damage, and smooth muscle cells (SMCs) excitability assays.

## 2.5 | Identifying whether ICS, SPE fractions, and their subfractions inhibit contractions of cultured muscularis preparations

The duodenojejunal and distal colon segments were removed from male SCD mice post euthanasia and placed immediately in ice-cold HEPES buffer ( $\text{mmol L}^{-1}$ : NaCl, 134; KCl, 6;  $\text{CaCl}_2$ , 2;  $\text{MgCl}_2$ , 1; HEPES, 10; and glucose, 10; pH 7.4) containing 2% penicillin-streptomycin (all reagents from Sigma, St. Louis, MO, USA). The samples were opened along the mesenteric border, pin-stretched in Sylgard-lined Petri dishes, washed with HEPES containing penicillin-streptomycin, and dissected to obtain muscularis externa (here after muscularis). Approximately, 1 cm long pieces of muscularis were cultured in Neurobasal A medium supplemented with B27 according to manufacturer's instructions (Thermo Fisher Scientific, Waltham, MA). Samples were cultured in ICS from male HFD mice (HFD-ICS), or male SCD mice (SCD-ICS), or HFD-SPE1, or SCD-SPE1. In addition, samples were cultured in HFD-ALC10-11, or SCD-ALC10-11, or HFD-MLC1, or SCD-MLC1. For control, tissues were cultured in 0.5  $\text{ng ml}^{-1}$  LPS (L4391), 30  $\mu\text{M}$  sodium palmitate (P9767), and 20 mM glucose (all from Sigma, St. Louis, MO, USA) or left untreated. All test substances were solubilized in culture media and filter sterilized with 0.22  $\mu\text{m}$  filters before use. Tissues were cultured in 24 well plates for 24 h at  $37^{\circ}\text{C}$ , 95% relative humidity and 5%  $\text{CO}_2$  concentration. 30-s long videos were recorded with a camera-equipped Nikon light microscope (Nikon, Melville, NY) using the 5 $\times$  objective lens after 1 h of equilibration (Time 0) and then 6, 12, and 24 h after adding test substances. Individuals not aware of treatments analyzed videos by counting the number

of contractions. Samples were immediately fixed for further analysis as described below. To measure contractions in distal colon muscularis, samples were loosely pinned in a tissue bath and cultured. The tissues were then transferred onto an inverted Nikon Ti-S microscope, washed for 10 min and then equilibrated in Krebs aerated with 95% O<sub>2</sub>/5% CO<sub>2</sub> for 30 min at 36.5°C. Videos of phasic contractions were captured with a Q-Imaging Micropublisher camera using 10× objective and analyzed by counting the number of contractions for 1 min.

## 2.6 | Identifying whether sera from HFD mice inhibit contractions of cultured muscularis preparations

Mouse sera were collected by terminal bleed as described previously<sup>8</sup> from male and female mice fed HFD or SCD for 8 weeks. Then, duodenojejunal muscularis were cultured in the presence of 1:50 diluted sera and the effect of sera on the frequency of muscularis contractions was measured as highlighted under Section 2.5.

## 2.7 | Immunohistochemistry analysis of nerve cell damage

Tissues were fixed overnight in 4% paraformaldehyde with 0.2% picric acid and washed in phosphate-buffered saline. Immunostaining was performed as previously described.<sup>8</sup> Neuronal nitric oxide synthase (nNOS) was used to localize nitrergic myenteric neurons. An anti-neuronal nuclear antibody 1 (ANNA1) was used as a pan neuronal marker. TNF $\alpha$  antibody was used to evaluate activation of inflammation in neurons. Oxidative stress was evaluated with anti-glutathione synthase antibody (GS). Nitrosative stress was studied with inducible nitric oxide synthase (iNOS) antibody. Tissues were stained with appropriate secondary antibodies and mounted, photographed, and analyzed as described previously.<sup>8</sup> Details about antibodies are in Table S1. Tissues were photographed using a Nikon DS-Qiz camera on a Nikon TiE inverted microscope using a 40× objective lens. Areas of ganglia were measured by tracing around ganglia using Nikon NIS-Elements software. The numbers of neurons were counted manually. Density indices were obtained by manually thresholding the stained areas within a ganglion and dividing it by the ganglionic area. A detailed procedure is in supplementary information.

## 2.8 | Determining whether ICS reduce inhibitory neuromuscular transmission

Approximately 1.5 cm long segments of the proximal distal colon were dissected to obtain muscularis samples as described previously.<sup>7</sup> Then, muscularis samples were treated with HFD-ICS, or SCD-ICS via Hepes, or left untreated for 6 h, at room temperature. Solutions were changed after 3 h. An inverted Nikon Ti-S microscope

was used to visualize tissues using 20× objective lens and measured inhibitory junction potentials (IJPs) in smooth muscle cells (SMCs) in circular layer by using sharp glass electrodes using established procedures.<sup>7,13</sup> See the supplementary information for the detailed procedure.

## 2.9 | Identifying whether ICS, SPE1 fractions, and its ALC10-11 subfractions inhibit the excitability of smooth muscle cells

Proximal distal colon muscularis were prepared and cultured in the presence of HFD-ICS or SCD-ICS or HFD-SPE1 or SCD-SPE1 or left untreated for 6 h as described above. In addition, samples were cultured under similar conditions in HFD-ALC10+11 or SCD-ALC10+11. Microelectrode recording was used to measure spontaneous slow wave and action potential activities in SMCs. SMCs health was analyzed during microelectrode recording and pictures taken with 20× objective lens and a Q-Imaging Micropublisher camera.

## 2.10 | Oxidative stress analysis by dihydroethidium staining

Superoxide levels were measured by quantifying the fluorescence of the superoxide marker DHE (Life Technologies, Carlsbad, CA)<sup>21</sup> as previously described.<sup>22</sup> Briefly, duodenal muscularis from nNOS-GCaMP6f mice were cultured for 12 h in HFD-ICS, or SCD-ICS, or HFD-ALC10-11, or SCD-ALC10-11, or LPS, or left untreated and then incubated with 2  $\mu$ M DHE dissolved in DMEM at 37°C for 1 h. DHE fluorescence levels were quantified in live ganglia after mounting samples and capturing images in 15–20 random fields of view with a 40× objective lens and Nikon DS-Qiz camera on a Nikon/Andor Spinning disk microscope. Images were analyzed with Nikon NIS-Elements software as described previously.<sup>8</sup>

## 2.11 | Quantification of inflammatory cytokines in culture medium

Duodenal muscularis were cultured in HFD-ICS or SCD-ICS or LPS or left untreated for 24 h and culture supernatants collected. Concentrations of inflammatory cytokines were measured using the multiplex magnetic bead-based immunoassay Luminex system and Milliplex mouse kits (Millipore, Billerica, MA, USA), according to the manufacturer's protocol. Data were analyzed using xPONENT 3.1 software (Austin, TX, USA).

## 2.12 | Statistical analysis

The effects of ICS on propulsive motility and muscle contractions were normalized by calculating the percentage of response

compared with basal propulsive velocities or basal muscularis contractions recorded in the same samples. Statistical analyses were performed using GraphPad Prism 5 (GraphPad software Inc, La Jolla, CA). A two-tailed unpaired Student's *t* test was used to compare means of SCD-ICS and HFD-ICS with means of untreated control samples. A parametric ANOVA with Tukey's post-hoc test was used to correct for multiple comparisons when analyzing data from more than two groups. Data are expressed as mean  $\pm$  standard error mean. Statistical significance between groups was determined at  $p < 0.05$ .

### 3 | RESULTS

#### 3.1 | Ileocecal supernatants from mice fed HFD (HFD-ICS) cause duodenal and colon dysmotility ex vivo

In motility studies, intraluminal perfusion of sterile and non-sterilized HFD-ICS from obese male mice with diabetic conditions and female mice without obesity or diabetic conditions rapidly decreased duodenal contractions and colonic pellet propulsion velocities (Figure 1A,B). SCD-ICS and a suspension of HFD did not affect duodenal or colon motility. The body weight, glucose, and insulin status of mice used to collect ICS were reported in a previous publication.<sup>13</sup> These results suggest that intestinal contents of mice fed HFD contain water-soluble antimotility molecules. Undigested HFD ingredients and microbial cells are not directly responsible for antimotility effects.

#### 3.2 | HFD-ICS inhibit contractions of duodenal and colon muscularis externa and damage smooth muscle cells

We next determined the effects of HFD-ICS from male mice on contractions of cultured muscularis from duodenum and distal colon. Compared with baseline contractions, untreated muscularis were contracting at a similar rate and had healthy looking SMCs after 24 h in culture. HFD-ICS completely blocked muscle contractions of both duodenal and colon muscularis after 12–24 h (Figure 2A,B; Video S1, Video S2, Video S3, and Video S4). In contrast, SCD-ICS, LPS, palmitate, LPS+palmitate combined, glucose, and a suspension of HFD in culture medium (not shown) did not affect muscularis contractions after 24 h. Additionally, HFD-ICS damaged muscularis cells causing swelling and some of the cells to fell off after 6–12 h. SCD-ICS did not cause SMCs swelling after 12 h (Figure 2C). These results suggest that HFD-ICS have toxic molecules that can disrupt intestinal muscle contractions by damaging neurons, SMCs, and other cells in the muscularis.

#### 3.3 | Sera from HFD mice inhibit contractions of duodenal muscularis

Since the likelihood of anterograde transport is low, we used sera to test the assumption that toxic molecules in ICS could affect

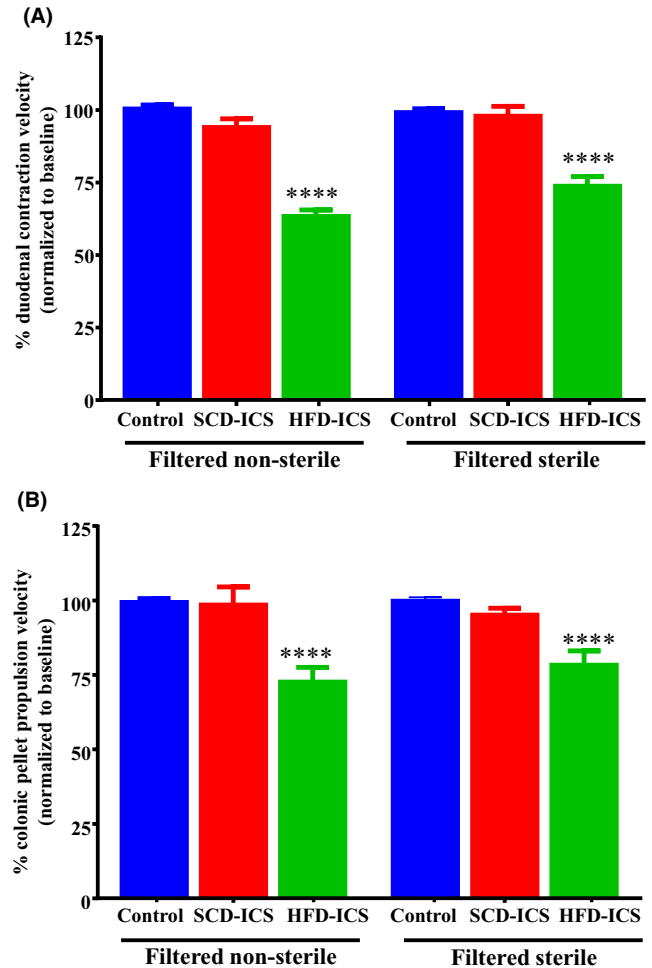


**FIGURE 1** HFD-ICS induces dysmotility in both duodenum and colon ex vivo. Duodenal contraction velocities (A) and colonic pellet propulsion velocities (B) were significantly reduced by HFD-ICS from both male and female mice after 5 min of perfusion compared with control and SCD-ICS. Filtering ICS with a 0.22  $\mu\text{m}$  filter, which removed microbial cells and other cells, did not change ICS effects on motility. Data were analyzed by one-way analysis of variance followed by Tukey's post-tests and are expressed as mean  $\pm$  SEM in all figures. Here and here after, numbers of animals for experiments were 5–10 per group. Statistical analysis was considered non-significant by  $p > 0.05$ . Statistical significance is denoted by symbols \**p* showing  $p \leq 0.05$ ; \*\**p* showing  $p \leq 0.01$ ; \*\*\**p* showing  $p \leq 0.001$ , and \*\*\*\**p*, showing  $p$  value  $\leq 0.0001$

proximal small intestine via circulation. Serum from male and female HFD mice decreased duodenal muscularis contractions (Figure S1).

#### 3.4 | HFD-ICS damage duodenal and colon nitrergic myenteric neurons

We determined whether HFD-ICS from male mice damage nitrergic myenteric neurons because nitrergic myenteric neurons, which

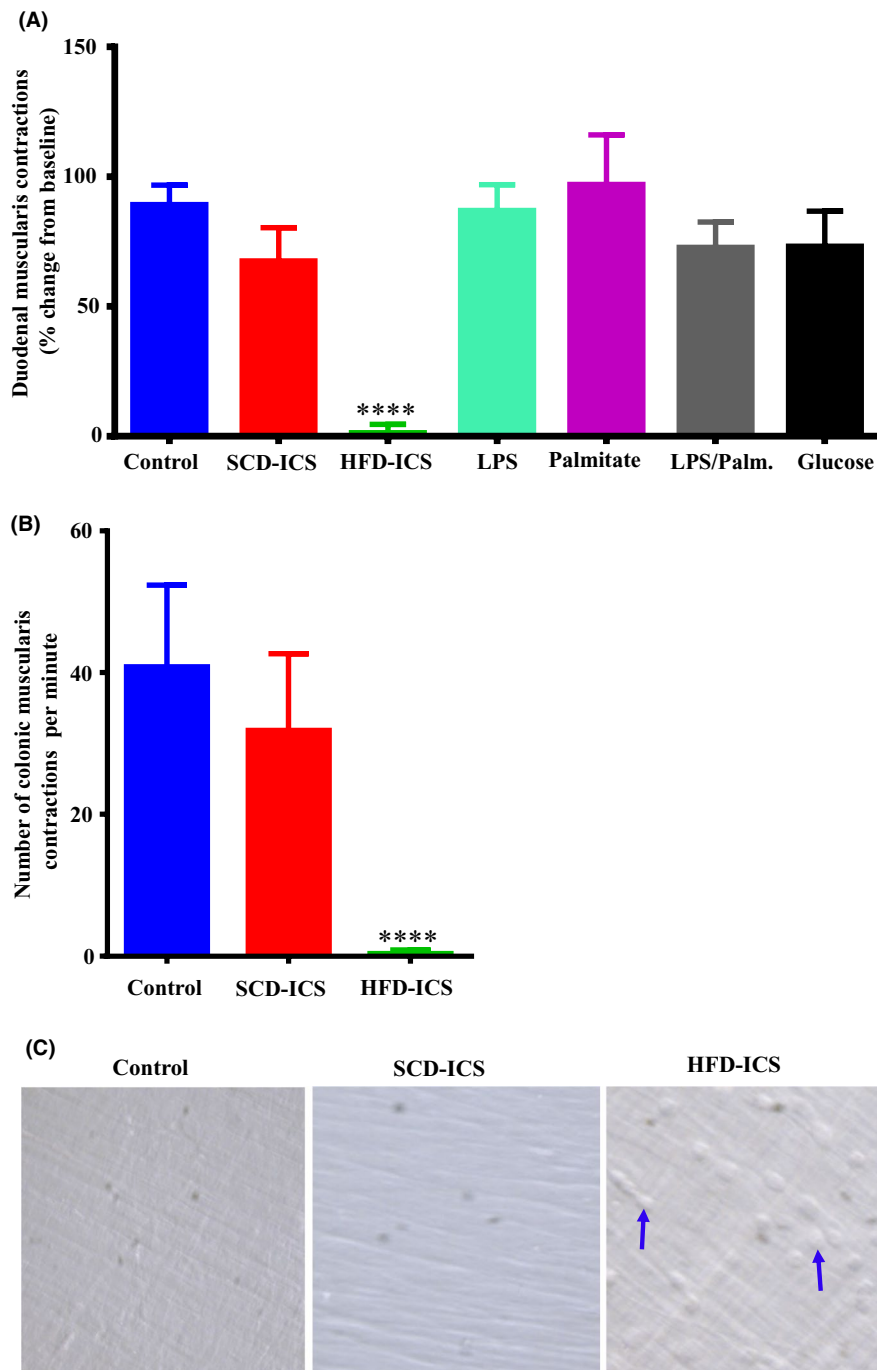


**FIGURE 2** HFD-ICS reduce contractions of small and large intestine muscularis preparations and damage smooth muscle cells (SMCs). After 24 h of culture, HFD-ICS from male mice reduced the number of contractions of muscularis preparations from duodenum (A) and distal colon (B) when compared to untreated control. SCD-ICS, LPS, palmitate, LPS/palmitate combination, and glucose did not affect muscularis contractions. Compared with untreated control and SCD-ICS, HFD-ICS caused swelling of SMCs suggesting it damaged these and other cells in muscularis preparation (C, arrows; 6 h)

are mainly inhibitory motor neurons are readily susceptible to injuries elicited by HFD and diabetes in animal models and diabetic humans.<sup>4,8</sup> After 24 h of culture, duodenal muscularis were fixed and stained by immunohistochemistry with ANNA1 and nNOS antibodies to label all myenteric neurons and nitrenergic myenteric neurons, respectively.<sup>23</sup> HFD-ICS reduced the percentage of nNOS

neurons (Figure 3A,B) and nNOS immunoreactivity (Figure S2) in myenteric ganglia like LPS, palmitate, and LPS/Palm. SCD-ICS did not affect myenteric nNOS neurons and nNOS immunoreactivity. These results suggest that there are neurotoxic molecules in the ileocecal contents of mice ingesting HFD, which damage nitrenergic myenteric neurons.

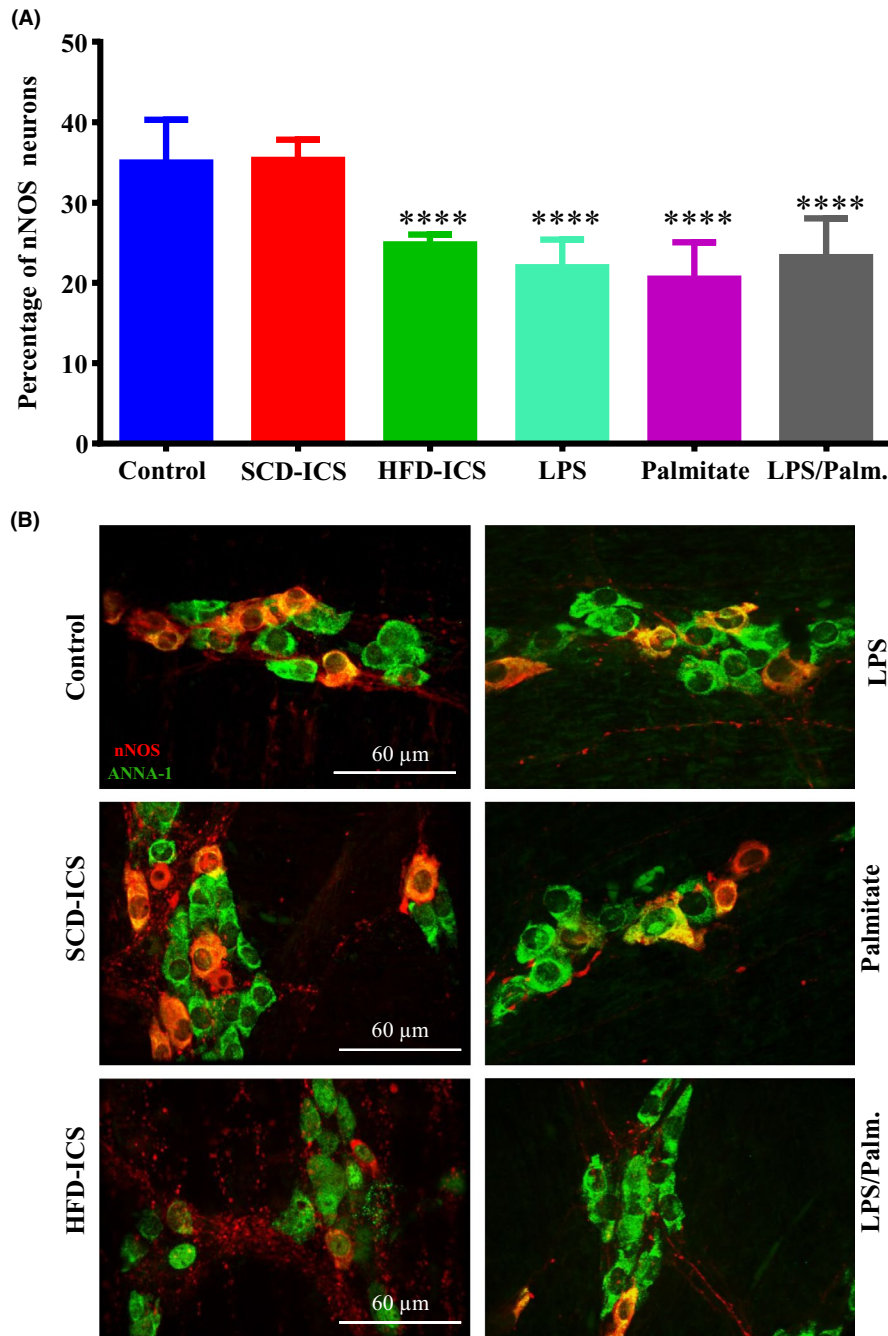


**FIGURE 3** HFD-ICS reduce the percentage of nNOS neurons in the myenteric plexus in duodenum. The percentage of nNOS neurons out of the total number of myenteric neurons (labeled with ANNA1) per ganglionic area was lower in samples treated with HFD-ICS from male mice for 24 h (A), which was similar to samples treated with LPS, palmitate, and LPS/palmitate when compared to untreated control and SCD-ICS. (B) Sample images showing overlays of nNOS (red) and ANNA1 (green) staining in duodenal myenteric ganglia of untreated control, SCD-ICS, HFD-ICS, LPS, palmitate, and LPS+palmitate (LPS/Palm.) treated samples

### 3.5 | HFD-ICS reduce inhibitory neuromuscular transmission

Diabetic-induced damage and HFD-induced damage to nitrenergic myenteric neurons diminish inhibitory neuromuscular transmission by decreasing the amplitude and duration of IJPs in SMCs.<sup>7,13</sup> To link HFD-ICS-induced dysmotility and impaired contractility to disrupted myenteric inhibitory neuromuscular transmission, we

studied the effects HFD-ICS from male mice have on IJPs in circular SMCs in distal colon muscularis. Compared with untreated controls and SCD-ICS, HFD-ICS reduced the amplitudes of the purinergic and nitrenergic components of IJPs but did not affect the overall duration of IJPs after 6 h (Figure 4A-C). Interestingly, SCD-ICS increased the durations of IJPs. These observations suggest that HFD-ICS have molecules that impair inhibitory neuromuscular transmission to circular SMCs. In contrast, molecules in



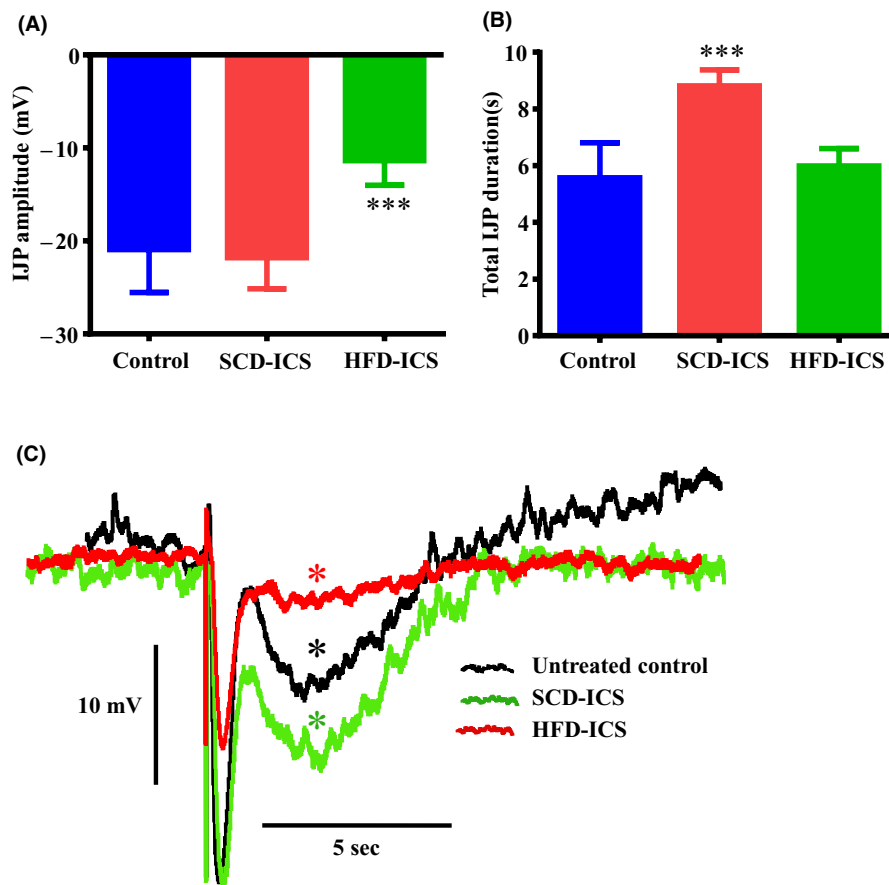


**FIGURE 4** HFD-ICS impairs intestinal inhibitory neuromuscular transmission to circular smooth muscle in distal colon. Treatment with HFD-ICS from male mice reduced the amplitudes of the fast purinergic and slow nitroergic (asterisks) components of IJPs (A, C) but did not change IJP durations (B) in circular smooth muscle cells in distal colon muscularis. SCD-ICS did not change IJP amplitudes but increased durations. (C) Traces of representative IJPs from untreated control, SCD-ICS, and HFD-ICS treated muscularis

SCD-ICS increase the durations of IJPs by enhancing the effects of NO and VIP.

### 3.6 | HFD-ICS inhibits the excitability of SMCs in the distal colon

The altered excitability of SMCs contributes to both HFD-induced dysmotility in animal models and diabetic GI dysmotility in humans.<sup>7</sup> However, whether molecules from intestinal contents could have a role in causing these effects has never been studied. We used intracellular microelectrode recording,<sup>24</sup> to determine whether HFD-ICS from male mice inhibit the excitability of SMCs by measuring slow wave and action potentials in circular SMCs in the distal colon. We observed that HFD-ICS depolarized SMCs after 6–12 h of culture and inhibited the discharge of slow waves and action potentials (Figure 5A–F). HFD-ICS disrupted the rhythmic firing of slow waves and action potentials in SMCs, causing prolonged quiescent periods. HFD-ICS also caused irregular bursting of action potentials on prolonged slow wave plateaus, a pattern resembling migrating motor complexes. Strikingly, the effects of HFD-ICS on the excitability of colonic SMCs matched the effects of HFD ingestion (Figure 5E,F).

In contrast, SCD ingestion and SCD-ICS did not affect the discharge of slow waves and action potentials (Figure 5C,D). These findings suggest that HFD-ICS contain toxic molecules that inhibit the excitability of SMCs.

### 3.7 | The neurotoxic and antimotility molecules in HFD-ICS are water-soluble

To chemically isolate and identify the neurotoxic antimotility molecules in HFD-ICS from male mice, we used bioactivity-guided SPE fractionation and HPLC subfractionation. This led us to discover that the aqueous, SPE1 and methanolic, SPE4 fractions from HFD-ICS mimicked the effects of HFD ingestion by reducing the number of duodenal contractions. However, SPE1 from HFD-ICS had stronger potency than SPE4 (Figure S3). Therefore, we used cultured duodenal muscularis to determine whether HPLC subfractions 10+11 of SPE1 from HFD mice (HFD-ALC10+11) and SCD mice (SCD-ALC10+11) inhibit muscularis contractions and damage nitroergic myenteric neurons. We compared them with HPLC subfraction 1 of SPE4 from HFD mice (HFD-MLC1) and SCD mice (SCD-MLC1). Like the HFD-ICS and HFD-SPE1, HFD-ALC10+11 entirely blocked

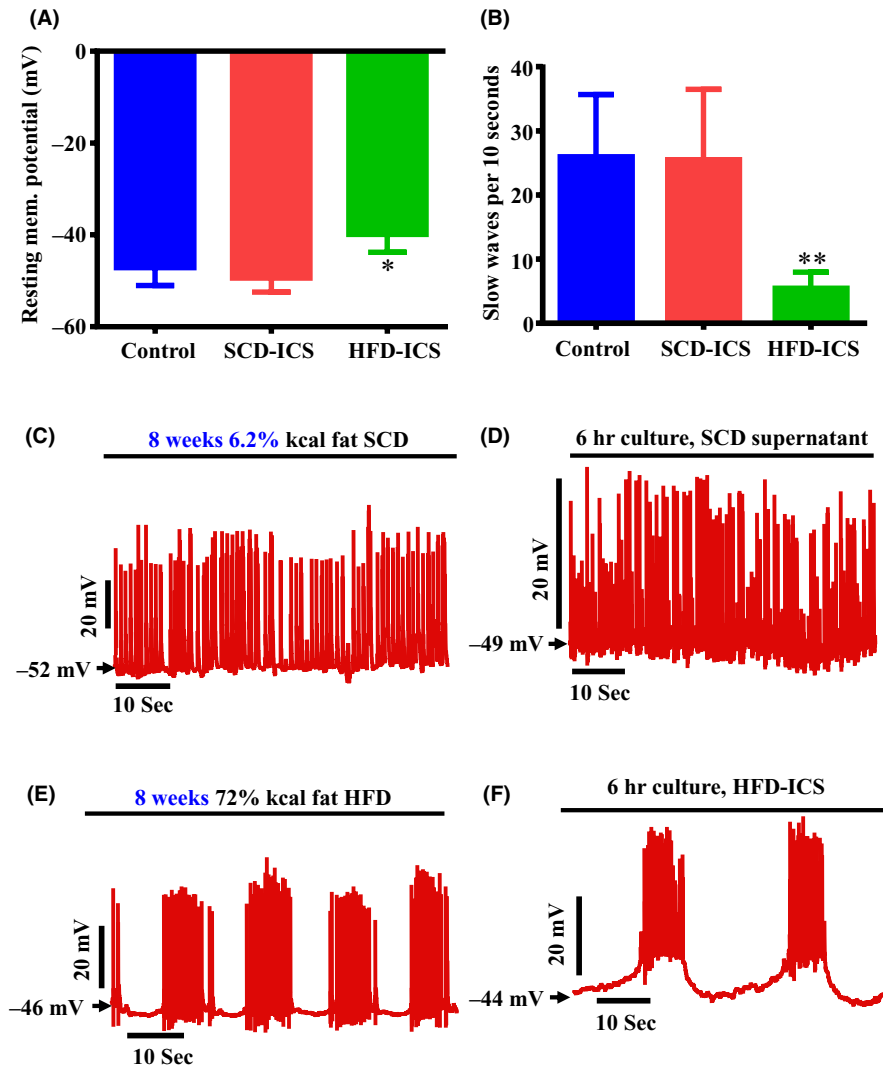


**FIGURE 5** HFD-ICS inhibits the excitability of smooth muscle cells. Compared to SCD-ICS, HFD-ICS from male mice depolarized resting membrane potentials in circular smooth muscle cells in distal colon muscularis (A) and reduced the frequency of slow waves (B) after 6 h of treatment. Compared to the rhythmic discharge of slow waves-action potentials from mice fed SCD for 8 weeks (C) and colon muscularis treated with SCD-ICS (D), both 8-week HFD ingestion (E) and HFD-ICS treatments (F) induced irregular discharge of slow waves-action potentials. They caused a bursting pattern of slow waves-action potentials and prolonged quiescent intervals

muscularis contractions (Figure 6A; Video S1, Video S2, Video S3, and Video S4), caused swelling of SMCs (Figure 6B), and reduced the percentage of nNOS neurons (Figure 6C,D). Additionally, HFD-ALC10+11 reduced intraganglionic nNOS immunoreactivity in myenteric ganglia after 24 h (Figure S4). Both HFD-MLC1 and SCD-MLC1 did not affect muscularis contractions or the percentage of nNOS neurons (Figure 6A,C), but reduced the nNOS immunoreactivity per ganglionic area (Figure S4). Unlike HFD-ALC10+11, SCD-ALC10+11 did not affect muscle contractions, damage SMCs or reduce the percentage of nNOS neurons (Figure 6A-D), but reduced ganglionic nNOS immunoreactivity (Figure S4).

Intracellular microelectrode recording<sup>24</sup> was used to determine whether HFD-ALC10+11 block smooth muscle contractions by inhibiting the excitability of SMCs in circular muscle layer in distal colon. Like, HFD ingestion and HFD-ICS, HFD-ALC10+11 depolarized and inhibited the excitability of SMCs after 6 h (Figure 6E,F).

Collectively, these results support the view that neurotoxic antimotility molecules in HFD-ICS are primarily water-soluble and can be isolated by using SPE and HPLC.

### 3.8 | HFD-ICS do not damage enteric neurons and smooth muscle via oxidative stress

Oxidative stress is the main factor that causes diabetic enteric neuropathy.<sup>4</sup> To determine whether HFD-ICS and its HFD-ALC10+11 damaged enteric neurons via oxidative stress duodenojejunal muscularis were cultured in HFD-ICS, or HFD-ALC10+11, or SCD-ICS, or SCD-ALC10+11, or LPS, or left untreated. One cohort of tissues was stained with dihydroethidium (DHE).<sup>22</sup> Another cohort was fixed and stained with an anti-glutathione synthase antibody to measure the expression of glutathione.<sup>25,26</sup> We observed that the DHE

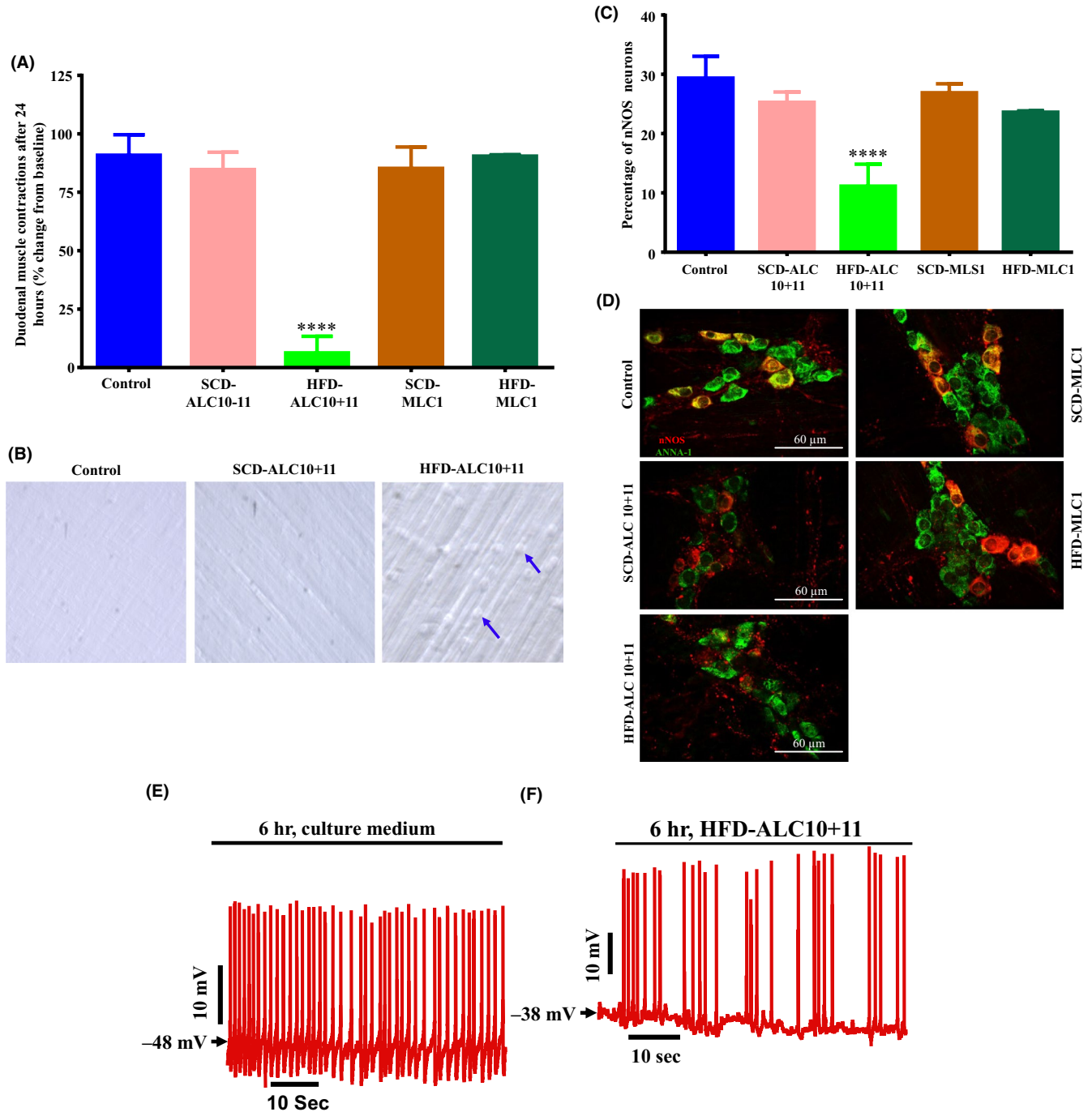


**FIGURE 6** Aqueous SPE fractions of HFD-ICS (HFD-SPE1) and its HPLC subfractions (HFD-ALC 10+11) block muscularis contractions by damaging smooth muscle cells and nNOS neurons and inhibiting the excitability of SMCs. Like HFD-ICS, HFD-SPE1 treatment blocked duodenal muscularis contractions after 24 h (shown in Figure S3). Like HFD-SPE1, culturing duodenal muscularis in its HPLC subfractions 10+11 (HFD-ALC 10+11) blocked contractions after 24 h (A). Also, similar to HFD-ICS and HFD-SPE1, HFD-ALC 10+11 damaged smooth muscle cells, evidenced by SMCs swelling after 6 h (B, arrows), and reduced the percentage of nNOS neurons out of the total number of myenteric neurons labeled with ANNA1 per ganglionic area after 24 h (C). Sample images (D) showing overlays of nNOS (red) and ANNA1 (green) staining in duodenum myenteric ganglia of control, SCD-ALC 10+11, HFD-ALC 10+11, and subfractions of methanolic SPE4 (SCD-MLC1 and HFD-MLC1) treated samples. Note severe damage and ANNA1 nuclear staining in HFD-ALC 10+11 treated sample. Finally, like HFD ingestion and HFD-ICS, HFD-ALC 10+11 depolarized resting membrane potentials in circular CSMs in distal colon muscularis preparations and inhibited the discharge of slow waves and action potentials (E-F, compare with Figure 5A-F)

stained area per ganglionic area was unchanged by the treatments above except LPS, which increased the DHE stained area after 12 h (Figure 7A,B). The total DHE stained area per field of view (DHE in

all cells) was also unaffected by all treatments except LPS (Figure S5). Additionally, the anti-glutathione synthase stained ganglionic area was not changed by either HFD-ICS or SCD-ICS but was increased

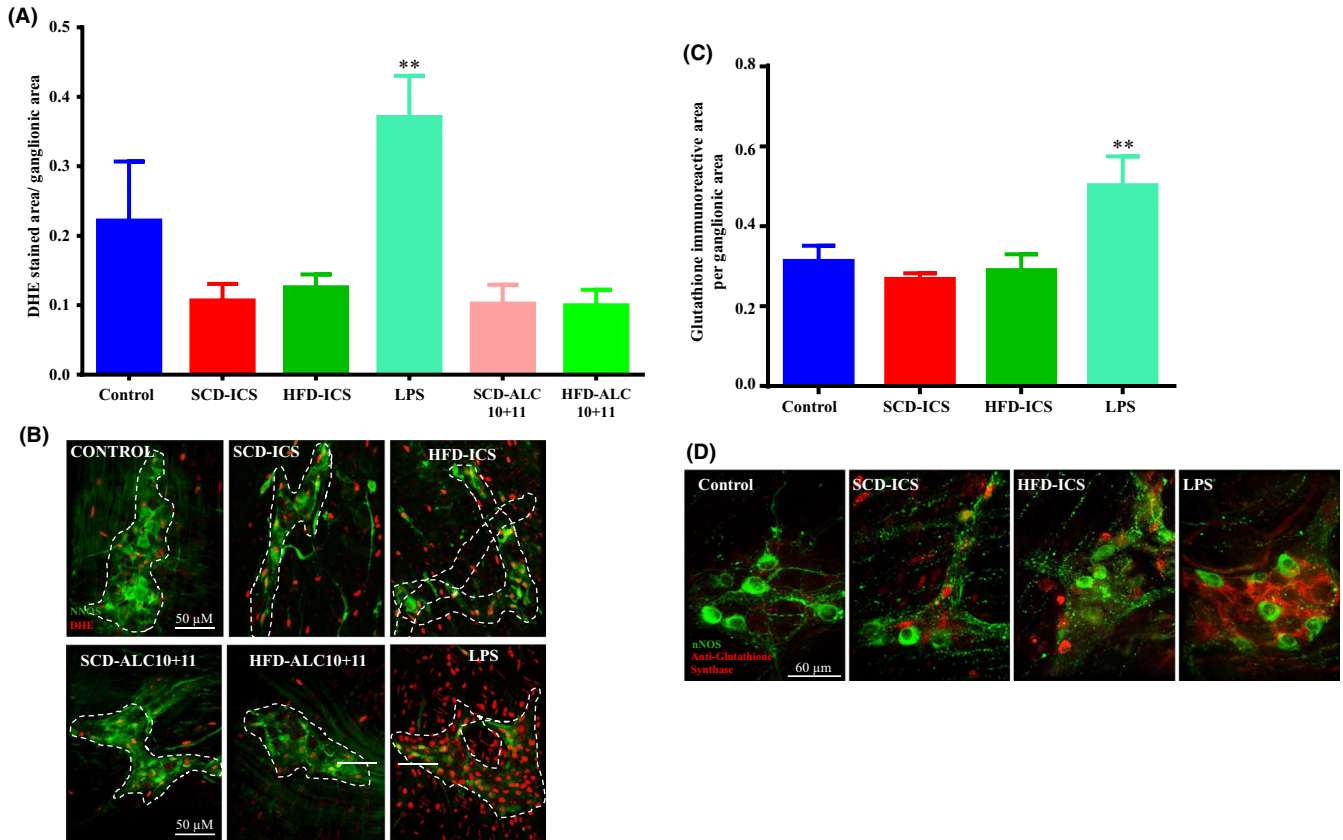


**FIGURE 7** HFD-ICS does not induce oxidative stress in myenteric neurons. HFD-ICS from male mice and HFD-ALC 10+11 subfractions did not increase the amount of DHE staining per ganglionic area (A). Sample images (B) showing nNOS (green) and DHE (red fluorescent) staining in duodenal myenteric ganglia of control, SCD-ICS, HFD-ICS, LPS, SCD-ALC 10+11, and HFD-ALC 10+11 treated samples. HFD-ICS did not affect anti-glutathione synthase immunoreactivity per ganglionic area (C). Sample images (D) showing that nNOS neurons (green immunoreactivity) rarely expressed anti-glutathione synthase (red) in duodenal myenteric ganglia of control, SCD-ICS, HFD-ICS, and LPS-treated samples. LPS increased DHE and anti-glutathione synthase staining suggesting it caused oxidative stress in myenteric ganglia

by LPS (Figure 7C,D). These results suggest that likely toxic molecules in HFD-ICS did not increase oxidative stress in ENS neurons after 12 h.

### 3.9 | HFD-ICS damage myenteric neurons via inflammation and nitrosative stress

Inflammation is one of the major pathways through which diabetic enteric neuropathy occurs and usually leads to oxidative and/or nitrosative stress.<sup>27</sup> We analyzed whether HFD-ICS induced inflammation and nitrosative stress in cultured duodenojejunal muscularis by measuring inflammatory cytokines and markers (TNF $\alpha$ , IL-6, MCP1, and PAI-1) in culture medium, and immunohistochemical staining for TNF $\alpha$  and iNOS after 24 h of culture. Compared with the untreated control samples and SCD-ICS, HFD-ICS and LPS increased TNF $\alpha$  concentration in culture medium (Figure 8A). However, unlike LPS, which dramatically increased IL-6, MCP1, and PAI-1 concentrations, HFD-ICS did not affect IL-6 (Figure 8B) and MCP1 but decreased the PAI-1 (Figure S6A,B). SCD-ICS did not affect the concentrations of TNF $\alpha$ , IL6, and MCP1 but lowered the concentration of PAI-1.

TNF $\alpha$  immunohistochemistry revealed that TNF $\alpha$  immunoreactivity was increased in myenteric ganglia after treatment with HFD-ICS compared with SCD-ICS and untreated control (Figure 8C,D). Like LPS, HFD-ICS treated samples had increased TNF $\alpha$ -immunoreactive neurons, but TNF $\alpha$ -immunoreactivity was more intense in LPS-treated samples. Similarly, compared with untreated control and SCD-ICS, LPS and HFD-ICS appeared to have more nNOS and non-nNOS neurons expressing iNOS. These data suggest that HFD-ICS induces TNF $\alpha$ -mediated neuroinflammation and nitrosative stress.

## 4 | DISCUSSION

The objective of this study was to determine whether ileocecal contents from male and female mice fed a HFD (HFD-ICS) contain molecules that impair intestinal motility by damaging and disrupting ENS neurons and smooth muscle functions. We observed that HFD-ICS contains yet to be identified neurotoxic and antimotility molecules that impair intestinal motility by damaging nitroergic myenteric neurons, disrupting inhibitory neuromuscular transmission,

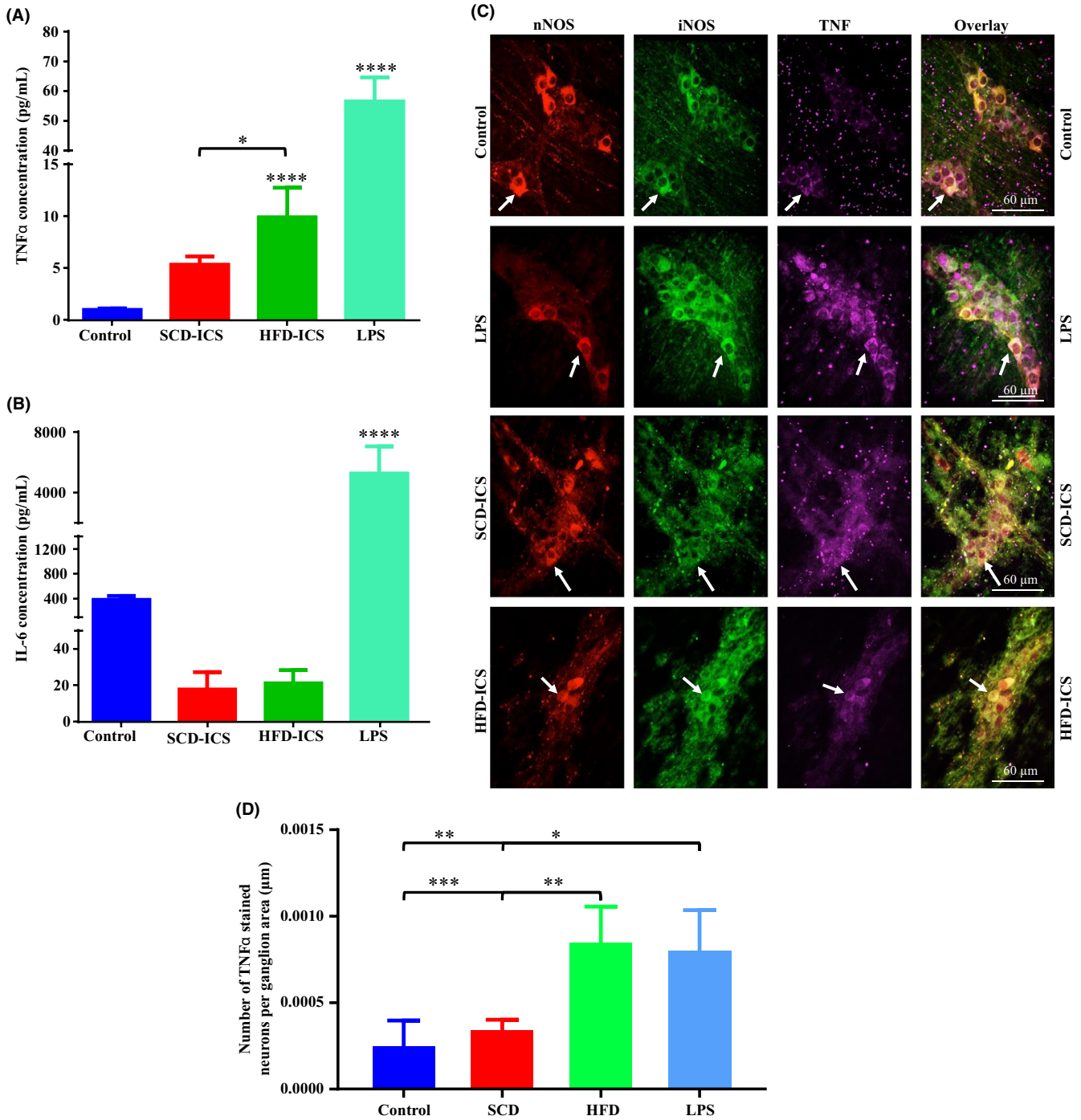


**FIGURE 8** HFD-ICS treatment induces the production of TNF $\alpha$  and causes nitrosative stress. After 24 h of treatment, like LPS, HFD-ICS from male mice resulted in higher concentrations of TNF $\alpha$  (A) in culture media but did not affect the concentrations of IL-6 (B). SPE1 fractions and ALC 10+11 subfractions were not tested. Images (C) to demonstrate qualitative analysis of inducible nitric oxide synthase (iNOS, green) and TNF $\alpha$  immunoreactivity (purple) in nNOS neurons (red) in control, SCD-ICS, HFD-ICS, and LPS-treated samples. Overlays show neurons expressing all markers (white arrows). Similar to LPS treatment, HFD-ICS treatment appeared to increase the number of neurons expressing TNF $\alpha$  and iNOS compared with untreated control samples. In addition, LPS increased both iNOS and TNF $\alpha$  compared with HFD-ICS and SCD-ICS. A summary graph (D) showing that HFD-ICS and LPS increased TNF $\alpha$  immunoreactive neurons compared with the untreated control and SCD-ICS treated samples

and by damaging SMCs and inhibiting their excitability. LPS, high glucose levels, and palmitate did not replicate these effects of HFD-ICS. Inflammation and nitrosative stress likely play key roles in the cellular mechanisms by which HFD-ICS damages ENS neurons and

smooth muscle. Our initial efforts to identify antimotility and neurotoxic molecules from HFD-ICS led us to discover that the aqueous SPE1 fraction of HFD-ICS and ALC10+11, two HPLC subfractions of HFD-SPE1 mimicked the effects of HFD-ICS in blocking muscle

contractions, damaging nitrergic myenteric neurons, and inhibiting the excitability of SMCs. This indicates that the neurotoxic and antimotility molecules in HFD-ICS can be isolated. Collectively, these results support our hypothesis that unknown antimotility and neurotoxic molecules in intestinal contents are involved in causing HFD-induced and diabetic GI neuropathy and dysmotility, and the view that diabetic ENS neuropathy and dysmotility occur before overt T2D.<sup>14,15</sup>

It is known that ENS neuropathy and motility-related disorders are complications of T2D<sup>4</sup> caused by hyperglycemia, dyslipidemia, oxidative/nitrosative stress, inflammation, advanced glycation end products, deficiency of neurotrophic factors, and gut microbiota changes.<sup>9,28–30</sup> However, current studies suggest that ENS neuropathy and dysmotility are triggered by lipotoxicity caused by palmitate and other dietary saturated fatty acids, and LPS from gut microbiota before hyperglycemia, insulin resistance, and overt T2D.<sup>12,13,17,28</sup> Still, literature is not very conclusive about all factors that trigger ENS neuropathy and dysmotility in T2D. The ENS and smooth muscle damaging and motility disruptive effects of HFD-ICS and aqueous fractions/subfractions from HFD male mice with T2D phenotype and HFD female mice without diabetic conditions suggest that antimotility and neurotoxic molecules in HFD-ICS are produced before insulin resistance. Our results support the view that factors which trigger ENS neuropathy and dysmotility originate from intestinal contents and provide evidence of the existence of unknown soluble neurotoxic and antimotility molecules in ileocecal contents of HFD mice other than LPS, palmitate, and glucose.<sup>9,12</sup> The inhibition of duodenal muscularis contractions by sera from HFD mice suggests that neurotoxic/antimotility molecules from ICS enter into circulation and may have a role in disrupting epithelial barrier function.<sup>31</sup> This supports future studies to determine whether molecules from the gut have a role in serum-induced neurotoxicity.<sup>32,33</sup> However, since sera of HFD mice have not been characterized, our results must be cautiously interpreted.

GI motility disorders in obesity and T2D are caused by ENS dysfunction and subsequent aberrant signaling.<sup>34</sup> Furthermore, dysmotility is associated with thickening and dysfunction of GI smooth muscle in both humans and animal models.<sup>4,7,35</sup> These pathologies cause decreased contractile force and peristaltic dyscoordination which lead to altered GI transit time.<sup>4,29,34,36</sup> The swelling and inflammation observed in our study suggest that toxic molecules in HFD-ICS could be involved in causing thickening and dysfunction of GI muscularis. Also, our results suggest that antimotility and neurotoxic molecules in HFD-ICS, its HFD-SPE1 and HFD-ALC10+11 are responsible for triggering disrupted GI motility by damaging nitrergic myenteric neurons and SMCs<sup>7</sup> causing decreased inhibitory neuromuscular transmission (IJP), NO-mediated interneuronal signaling, and disrupted excitability of SMCs. In contrast, we postulate that SCD-ICS prolonged IJP durations by enhanced nitric oxide (NO) signaling to SMCs.<sup>7</sup> This is because unpublished observations from the Balemba laboratory suggest that SCD-ICS appeared to increase intramuscular nNOS varicosities. Analyzing the effect of HFD-ICS

and SCD-ICS on NO release from intestinal muscularis is required to confirm this idea.

We previously showed that HFD ingestion impairs duodenal motility in male and female mice even though female mice did not have diabetic conditions.<sup>13</sup> In diabetic humans and animals, the ENS in the proximal intestine is thought to be damaged first leading to postprandial duodenal hypercontractility.<sup>37,38</sup> Increasing LPS concentration in the colon by enema can evoke inflammation in the small intestine.<sup>39</sup> Therefore, we hypothesized that toxins in ICS can affect small intestine. The ability to see and count duodenal muscularis contractions with unaided eyes inspired us to use duodenojejunal muscularis to screen ICS and derived fractions to test it. It has been shown that LPS inhibits intestinal contractions in rodents but C57BL/6J mice are relatively resistant to LPS-induced impaired intestinal motility/contractility.<sup>40</sup> The observation that LPS treatment did not disrupt muscle contractions despite inducing inflammation, oxidative stress, and loss of neurons match these previous findings and suggest a need to include different strains of mice in future studies.<sup>40</sup> Still, the robust differences between HFD-ICS and molecules that are known to cause damage to ENS and disrupt motility suggest the presence of novel toxic molecules in the intestinal content of HFD mice. Future studies will focus on chemical identification of toxic molecules and the mechanisms by which HFD-ICS and isolated molecules disrupt neurotransmission and the excitability of SMCs.

In diabetic ENS neuropathy, necrosis and loss of ENS neurons are thought to be caused by oxidative/nitrosative stress and neuroinflammation.<sup>4,41</sup> LPS and hyperglycemia cause apoptosis of ENS neurons by activating these pathways.<sup>12,25</sup> In this study, it was evident that HFD-ICS increased TNF- $\alpha$  and nitrosative stress in neurons, supporting the idea that unknown molecules in HFD-ICS and SPE1 damage myenteric neurons through activation of neuroinflammation and nitrosative stress. Our results support findings showing that colonizing the rectum of healthy germ-free mice with fecal slurries from conventional mice fed HFD activates inflammation.<sup>42</sup> The fact that HFD-ICS did not affect DHE and GS was unexpected, because of the significant loss of nitrergic myenteric neurons and oxidative stress usually occurs in conjunction with inflammation.<sup>27</sup> We cannot confidently rule out the involvement of oxidative stress in the nerve damage induced by toxic molecules in HFD-ICS without thoroughly analyzing the time- and concentration-dependent effects—especially by using isolated toxic molecules. Further studies are therefore necessary to determine molecular mechanisms by which HFD-ICS, HFD-SPE1, and the isolated antimotility and neurotoxic molecules damage ENS neurons and SMCs. For instance, investigating the role of NF- $\kappa$ B and Nrf2 pathways, two important pathways that control oxidative stress and inflammation and mediate cellular homeostasis<sup>27</sup> is necessary. Studies focused on the effects of HFD-ICS on cholinergic and other classes of enteric neurons will provide insights into the mechanism of action.

Could our findings be implicated in the pathophysiology of other neurodegenerative and smooth muscle illnesses linked to

gut microbiota, mucosal barrier dysfunction, and GI inflammation? HFD ingestion changes the composition of gut microbiota and causes intestinal inflammation, disrupted mucosal barrier function, and LPS endotoxemia.<sup>14</sup> It also results in increased GI transit, and damage to enteric neurons.<sup>8,12,13</sup> These abnormalities occur in prediabetes and diabetic patients, and disrupted mucosal barrier promotes an abnormal passage of luminal substances into the intestinal wall.<sup>43,44</sup> We recently reported that HFD-induced changes to gut microbiota composition play a role in HFD-induced neuropathy and dysmotility.<sup>45</sup> Additionally, changes to gut microbiota composition have been linked to the production of toxic molecules causing decreased colonic muscle contractility in irritable bowel disease,<sup>46</sup> and visceral hypersensitivity in colicky infants.<sup>47</sup> Furthermore, there is an increasing number of studies providing evidence to link CNS neurologic diseases, notably autism spectrum disorder, Parkinson's disease, and Alzheimer's disease to altered gut microbiota and GI dysfunctions.<sup>48,49</sup> Patients commonly manifest by intestinal dysmotility and enteric neuropathy, altered gut microbiota composition, intestinal inflammation, disrupted mucosal barrier function, and neuroinflammation.<sup>48,50,51</sup> However, toxic molecules from the GI lumen are largely unknown. It is likely that neurotoxic and antimotility molecules in HFD-ICS and HFD-SPE1 are derived from altered gut microbial communities<sup>45</sup> and can cross the disrupted mucosal barrier and injure cells in the GI wall and other body organs. Whether this is the case in other GI disorders or CNS neurologic diseases remains to be determined. Therefore, future studies to identify toxic molecules from HFD-ICS and supernatants from human intestinal contents, and their potential link to the gut microbiota are crucial.

## 5 | CONCLUSIONS

In conclusion, our study strongly suggests that HFD ingestion causes production of unknown antimotility and neurotoxic molecules in the gut. These molecules are likely produced early due to changes in the gut microbial community and could have a role in triggering enteric neuropathy, SMCs injury, and dysmotility, before the onset of T2D symptoms. These findings highlight the significance of identifying specific neurotoxic and antimotility molecules in ileocecal contents of HFD mice due to their potential essential role in GI motility disorders, diabetes, and other diseases associated with injury to neurons or SMCS. Furthermore, these molecules can potentially be used as biomarkers for the early detection of such diseases. Finally, our results warrant proof-of-concept in vivo studies in healthy mice and translational analysis of ICS from prediabetic and T2D humans.

## ACKNOWLEDGMENTS

We would like to thank Laboratory Animal Research Facility staff for assistance with animal care, and Roan Wilson and Ann Norton (Optical Imaging Core) for assistance with imaging and/or data

analysis. We thank Drs Tanya Miura and Lee Fortunato for assistance with tissue culture, Drs Larry Forney and Armando McDonald for advice on experimental design, and Drs Vanda A. Lennon and David R. Linden for assistance with ANNA1 antibody.

## DISCLOSURE

The authors have no competing interests.

## AUTHOR CONTRIBUTIONS

YN and OBB designed experiments. YN, HH, TOM, TDS, and OBB developed methodologies; YN, CRB, SK, JN, KKC, GM, CM, AY, FP, JC, HH, TOM, TDS, and OBB performed the research and acquired data. YN and OB analyzed and interpreted data. YN, TDS, TOM, HH, and OBB wrote, reviewed and revised the manuscript. TDS, HH, TOM, TH, and OBB supervised the study.

## ORCID

Yvonne Nyavor  <https://orcid.org/0000-0002-7559-3803>

Heino M. Heyman  <https://orcid.org/0000-0003-0941-2506>

Onesmo B. Balemba  <https://orcid.org/0000-0003-1034-2242>

## REFERENCES

1. Guariguata L, Whiting DR, Hambleton I, Beagley J, Linnenkamp U, Shaw JE. Global estimates of diabetes prevalence for 2013 and projections for 2035. *Diabetes Res Clin Pract.* 2014;103(2):137-149.
2. Singh R, Kishore L, Kaur N. Diabetic peripheral neuropathy: current perspective and future directions. *Pharmacol Res.* 2014;80:21-35.
3. Smyth S, Heron A. Diabetes and obesity: the twin epidemics. *Nat Med.* 2006;12(1):75-80.
4. Yarandi SS, Srinivasan S. Diabetic gastrointestinal motility disorders and the role of enteric nervous system: current status and future directions. *Neurogastroenterol Motil.* 2014;26(5):611-624.
5. Feldman M, Schiller LR. Disorders of gastrointestinal motility associated with diabetes mellitus. *Ann Intern Med.* 1983;98(3):378-384.
6. Krishnan B, Babu S, Walker J, Walker AB, Pappachan JM. Gastrointestinal complications of diabetes mellitus. *World J Diabetes.* 2013;4(3):51.
7. Bhattarai Y, Fried D, Gulbransen B, et al. High-fat diet-induced obesity alters nitric oxide-mediated neuromuscular transmission and smooth muscle excitability in the mouse distal colon. *Am J Physiol Liver Physiol.* 2016;311(2):G210-G220.
8. Stenkamp-Strahm CM, Kappmeyer AJ, Schmalz JT, Gericke M, Balemba O. High-fat diet ingestion correlates with neuropathy in the duodenum myenteric plexus of obese mice with symptoms of type 2 diabetes. *Cell Tissue Res.* 2013;354(2):381-394.
9. Anitha M, Gondha C, Sutliff R, et al. GDNF rescues hyperglycemia-induced diabetic enteric neuropathy through activation of the PI3K/Akt pathway. *J Clin Invest.* 2006;116(2):344-356.
10. Vincent AM, Russell JW, Low P, Feldman EL. Oxidative stress in the pathogenesis of diabetic neuropathy. *Endocr Rev.* 2004;25(4):612-628.
11. Bagyánszki M, Bódi N. Diabetes-related alterations in the enteric nervous system and its microenvironment. *World J Diabetes.* 2012;3(5):80-93.
12. Reichardt F, Chassaing B, Nezami BG, et al. Western diet induces colonic nitrergic myenteric neuropathy and dysmotility in mice via saturated fatty acid- and lipopolysaccharide-induced TLR4 signaling. *J Physiol.* 2017;595(5):1831-1846.
13. Nyavor Y, Estill R, Edwards H, et al. Intestinal nerve cell injury occurs prior to insulin resistance in female mice ingesting a high-fat diet. *Cell Tissue Res.* 2019;376(3):325-340.

14. Cani PD, Amar J, Iglesias MA, et al. Metabolic endotoxemia initiates obesity and insulin resistance. *Diabetes*. 2007;56(7):1761-1772.
15. Voss U, Sand E, Olde B, Ekblad E. Enteric neuropathy can be induced by high fat diet in vivo and palmitic acid exposure in vitro. *PLoS One*. 2013;8(12):e81413.
16. Aziz Q, Doré J, Emmanuel A, Guarner F, Quigley EMM. Gut microbiota and gastrointestinal health: current concepts and future directions. *Neurogastroenterol Motil*. 2013;25(1):4-15.
17. Nyavor YEA, Balemba OB. Diet-induced dysmotility and neuropathy in the gut precedes endotoxaemia and metabolic syndrome: the chicken and the egg revisited. *J Physiol*. 2017;595(5):1441-1442.
18. Islam MS. Animal models of diabetic neuropathy: progress since 1960s. *J Diabetes Res*. 1960s;2013:149452.
19. Everard A, Lazarevic V, Gaia N, et al. Microbiome of prebiotic-treated mice reveals novel targets involved in host response during obesity. *ISME J*. 2014;8(10):2116-2130.
20. Stark T, Hofmann T. Isolation, structure determination, synthesis, and sensory activity of N-phenylpropenoyl-L-amino acids from Cocoa (*Theobroma cacao*). *J Agric Food Chem*. 2005;53(13):5419-5428.
21. Benov L, Szejnberg L, Fridovich I. Critical evaluation of the use of hydroethidine as a measure of superoxide anion radical. *Free Radic Biol Med*. 1998;25(7):826-831.
22. Brown IAM, McClain JL, Watson RE, Patel BA, Gulbransen BD. Enteric glia mediate neuron death in colitis through purinergic pathways that require connexin-43 and nitric oxide. *Cell Mol Gastroenterol Hepatol*. 2016;2(1):77-91.
23. Qu Z-D, Thacker M, Castelucci P, Bagyánszki M, Epstein ML, Furness JB. Immunohistochemical analysis of neuron types in the mouse small intestine. *Cell Tissue Res*. 2008;334(2):147-161.
24. France M, Bhattarai Y, Galligan JJ, Xu H. Impaired propulsive motility in the distal but not proximal colon of BK channel  $\beta$ 1-subunit knockout mice. *Neurogastroenterol Motil*. 2012;24(9):e450-e459.
25. Chandrasekharan B, Anitha M, Blatt R, et al. Colonic motor dysfunction in human diabetes is associated with enteric neuronal loss and increased oxidative stress. *Neurogastroenterol Motil*. 2011;23(2):131-e26.
26. Brown IAM, Gulbransen BD. The antioxidant glutathione protects against enteric neuron death in situ, but its depletion is protective during colitis. *Am J Physiol Liver Physiol*. 2018;314(1):G39-G52.
27. Sandireddy R, Yerra VG, Areti A, Komirishetty P, Kumar A. Neuroinflammation and oxidative stress in diabetic neuropathy: futuristic strategies based on these targets. *Int J Endocrinol*. 2014;2014:674987.
28. Anitha M, Reichardt F, Tabatabavakili S, et al. Intestinal dysbiosis contributes to the delayed gastrointestinal transit in high-fat diet fed mice. *Cell Mol Gastroenterol Hepatol*. 2016;2(3):328-339.
29. Gotfried J, Priest S, Schey R. Diabetes and the small intestine. *Curr Treat Options Gastroenterol*. 2017;15(4):490-507.
30. Abrahamsson H. Gastrointestinal motility disorders in patients with diabetes mellitus. *J Intern Med*. 1995;237(4):403-409.
31. Oliveira RB, Canuto LP, Collares-Buzato CB. Intestinal luminal content from high-fat-fed prediabetic mice changes epithelial barrier function in vitro. *Life Sciences*. 2019;216:10-21.
32. Srinivasan S, Stevens MJ, Sheng H, Hall KE, Wiley JW. Serum from patients with type 2 diabetes with neuropathy induces complement-independent, calcium-dependent apoptosis in cultured neuronal cells. *Journal of Clinical Investigation*. 1998;102(7):1454-1462.
33. Towns R, Kabeya Y, Yoshimori T, Guo C, Shangguan Y, Hong S, Kaplan M, Klionsky DJ, Wiley JW. Sera from patients with type 2 Diabetes and Neuropathy Induce Autophagy and Colocalization with Mitochondria in SY5Y cells. *Autophagy*. 2005;1(3):163-170.
34. Ohlsson B, Melander O, Thorsson O, Olsson R, Ekberg O, Sundkvist G. Oesophageal dysmotility, delayed gastric emptying and autonomic neuropathy correlate to disturbed glucose homeostasis. *Diabetologia*. 2006;49(9):2010-2014.
35. Farrugia G. Histologic changes in diabetic gastroparesis. *Gastroenterol Clin North Am*. 2015;44(1):31-38.
36. Horváth VJ, Putz Z, Izbéki F, et al. Diabetes-related dysfunction of the small intestine and the colon: focus on motility. *Curr Diab Rep*. 2015;15(11):94.
37. Fournel A, Drougard A, Duparc T, et al. Apelin targets gut contraction to control glucose metabolism via the brain. *Gut*. 2017;66(2):258-269.
38. Abot A, Lucas A, Bautzova T, et al. Galanin enhances systemic glucose metabolism through enteric Nitric Oxide Synthase-expressed neurons. *Mol Metab*. 2018;10:100-108.
39. Im E, Riegler FM, Pothoulakis C, Rhee SH. Elevated lipopolysaccharide in the colon evokes intestinal inflammation, aggravated in immune modulator-impaired mice. *American Journal of Physiology-Gastrointestinal and Liver Physiology*. 2012;303(4):G490-G497.
40. Killoran KE, Miller AD, Uray KS, et al. Role of innate immunity and altered intestinal motility in LPS- and MnCl<sub>2</sub>-induced intestinal intussusception in mice. *Am J Physiol Liver Physiol*. 2014;306(5):G445-G453.
41. Giacco F, Brownlee M. Oxidative stress and diabetic complications. *Circ Res*. 2010;107(9):1058-1070.
42. Ding S, Chi MM, Scull BP, et al. High-fat diet: bacteria interactions promote intestinal inflammation which precedes and correlates with obesity and insulin resistance in mouse. *PLoS One*. 2010;5(8):e12191.
43. Jayashree B, Bibin YS, Prabhu D, et al. Increased circulatory levels of lipopolysaccharide (LPS) and zonulin signify novel biomarkers of proinflammation in patients with type 2 diabetes. *Mol Cell Biochem*. 2014;388(1-2):203-210.
44. Cani PD, Bibiloni R, Knauf C, et al. Changes in gut microbiota control metabolic endotoxemia-induced inflammation in high-fat diet-induced obesity and diabetes in mice. *Diabetes*. 2008;57(6):1470-1481.
45. Nyavor Y, Brands CR, May G, Kuther S, Nicholson J, Tiger K, Tesnohlídek A, Yasuda A, Starks K, Litvinenko D, Linden DR, Bhattarai Y, Kashyap PC, Forney LJ, Balemba OB. High-fat diet-induced alterations to gut microbiota and gut-derived lipoteichoic acid contributes to the development of enteric neuropathy. *Neurogastroenterology & Motility*. 2020;32(7):e13838.
46. Guarino MP, Barbara G, Cicenia A, et al. Supernatants of irritable bowel syndrome mucosal biopsies impair human colonic smooth muscle contractility. *Neurogastroenterol Motil*. 2017;29(2):1-9.
47. Eutamène H, Garcia-Rodenas CL, Yvon S, et al. Luminal contents from the gut of colicky infants induce visceral hypersensitivity in mice. *Neurogastroenterol Motil*. 2017;29(4):e12994.
48. Roy Sarkar S, Banerjee S. Gut microbiota in neurodegenerative disorders. *J Neuroimmunol*. 2019;328:98-104.
49. Jolanta Wasilewska J, Klukowski M. Gastrointestinal symptoms and autism spectrum disorder: links and risks – a possible new overlap syndrome. *Pediatr Heal Med Ther*. 2015;153:153-166.
50. Cersosimo MG, Benarroch EE. Pathological correlates of gastrointestinal dysfunction in Parkinson's disease. *Neurobiol Dis*. 2012;46(3):559-564.
51. Chalazonitis A, Rao M. Enteric nervous system manifestations of neurodegenerative disease. *Brain Res*. 2018;1693:207-213.

## SUPPORTING INFORMATION

Additional supporting information may be found online in the Supporting Information section.

**How to cite this article:** Nyavor Y, Brands CR, Nicholson J, et al. Supernatants of intestinal luminal contents from mice fed high-fat diet impair intestinal motility by injuring enteric neurons and smooth muscle cells. *Neurogastroenterology & Motility*. 2021;33:e13990. <https://doi.org/10.1111/nmo.13990>